

See discussions, stats, and author profiles for this publication at: <https://www.researchgate.net/publication/6932448>

# Comparative Study of the Thermodynamics and Kinetics of the Ion Transfer Across the Liquid|Liquid Interface by Means of Three-Phase Electrodes

ARTICLE in THE JOURNAL OF PHYSICAL CHEMISTRY B · AUGUST 2005

Impact Factor: 3.3 · DOI: 10.1021/jp0519969 · Source: PubMed

CITATIONS

27

READS

13

## 6 AUTHORS, INCLUDING:



François Quentel

Université de Bretagne Occidentale

106 PUBLICATIONS 1,062 CITATIONS

SEE PROFILE



Valentin Mirceski

Ss. Cyril and Methodius University

102 PUBLICATIONS 1,600 CITATIONS

SEE PROFILE



Mitko Mladenov

45 PUBLICATIONS 149 CITATIONS

SEE PROFILE



Catherine Elleouet

Université de Bretagne Occidentale

43 PUBLICATIONS 462 CITATIONS

SEE PROFILE

# Comparative Study of the Thermodynamics and Kinetics of the Ion Transfer Across the Liquid|Liquid Interface by Means of Three-Phase Electrodes

François Quentel,<sup>†</sup> Valentin Mirčeski,<sup>\*,‡</sup> Maurice L'Her,<sup>†</sup> Mitko Mladenov,<sup>§</sup> Fritz Scholz,<sup>||</sup> and Catherine Elleouet<sup>†</sup>

Laboratoire de Chimie Analytique, UMR-CNRS 6521, Université de Bretagne Occidentale, 6, avenue Victor Le Gorgeu, C.S. 93837, 29238 BREST Cedex 3, France, Institute of Chemistry, Faculty of Natural Sciences and Mathematics, "Sv. Kiril i Metodij" University, P.O. Box 162, 1000 Skopje, Republic of Macedonia, Institute of Biology, Faculty of Natural Sciences and Mathematics, "Sv. Kiril i Metodij" University, P.O. Box 162, 1000 Skopje, Republic of Macedonia, and Institut für Chemie und Biochemie, University in Greifswald, Soldmannstrasse 23, D-17489 Greifswald, Germany

Received: April 18, 2005

A comparative study of the behavior of different sorts of three-phase electrodes applied for assessing the thermodynamics and kinetics of the ion transfer across the liquid|liquid (L|L) interface is presented. Two types of three-phase electrodes are compared, that is, a paraffin-impregnated graphite electrode at the surface of which a macroscopic droplet of an organic solvent is attached and an edge pyrolytic graphite electrode partly covered with a very thin film of the organic solvent. The organic solvent contains either decamethylferrocene or lutetium bis(tetra-*tert*-butylphthalocyaninato) as a redox probe. The role of the redox probe, the type of the electrode material, the mass transfer regime, and the effect of the uncompensated resistance are discussed. The overall electrochemical process at both three-phase electrodes proceeds as a coupled electron–ion transfer reaction. The ion transfer across the L|L interface, driven by the electrode reaction of the redox compound at the electrode|organic solvent interface, is independent of the type of redox probe. The ion transfer proceeds without involving any chemical coupling between the transferring ion and the redox probe. Both types of three-phase electrodes provide consistent results when applied for measuring the energy of the ion transfer. Under conditions of square-wave voltammetry, the coupled electron–ion transfer at the three-phase electrode is a quasireversible process, exhibiting the property known as "quasireversible maximum". The overall electron–ion transfer process at the three-phase electrode is controlled by the rate of the ion transfer. It is demonstrated for the first time that the three-phase electrode in combination with the quasireversible maximum is a new tool for assessing the kinetics of the ion transfer across the L|L interface.

## 1. Introduction

The importance of the ion transfer across the interface between two immiscible liquids is well recognized and has been intensively studied over decades.<sup>1</sup> The charge transfer across the aqueous|organic solution interface represents a simplified model for understanding complex charge transfer reactions across the biomembranes, which play a key role in the living cells of all organisms. In the past few years, the three-phase electrode emerged as a simple and powerful tool for studying the thermodynamics of ion transfer across the liquid|liquid (L|L) interface.<sup>2–5</sup> This system consists of a graphite electrode modified by a droplet of an electrochemically inactive water-immiscible organic solvent (O) containing a neutral redox probe. The electrode is immersed in an aqueous electrolyte solution (W) and used in a conventional three-electrode configuration. Upon electrochemical transformation of the redox probe in the organic medium, the charge neutrality requires an ion transfer from the aqueous phase.

The three-phase electrode operates without any added electrolyte in the organic phase, which appears to be its main

advantage. Despite this fact, a lot of studies demonstrated that the three-phase electrode in combination with a sensitive and fast voltammetric technique such as square-wave voltammetry (SWV)<sup>3–6</sup> provides a well-defined voltammetric response enabling precise measurement of the formal potential of the system. This is primarily enabled by the three-phase boundary line, that is, the line along which the organic phase provides the redox active material, the aqueous phase supplies charge compensating counterions, whereas the electrode serves as a source or a sink of electrons.<sup>7</sup> Once the reaction starts along the three-phase boundary line, it expands further on in the edge region of the droplet.<sup>7,8</sup> In the course of the voltammetric experiment, the conductivity of the organic phase rapidly increases due to the formation of the charged species in the organic phase and to the simultaneous ingress of an equivalent amount of counterions from the aqueous phase. Consequently, despite the absence of the electrolyte in the organic phase, the uncompensated resistance does not affect the voltammetric response significantly.

Most frequently, the three-phase electrode is assembled of a paraffin-impregnated graphite electrode (PIGE), modified with a single macroscopic droplet of a nitrobenzene (NB) solution containing decamethylferrocene (DMFC) as a redox probe (Scheme 1).<sup>2–4</sup> Upon oxidation of DMFC to the monovalent hydrophobic decamethylferrocenium cation (DMFC<sup>+</sup>), the

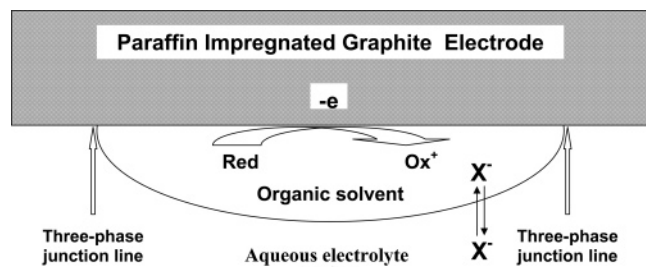
\* Corresponding author. E-mail: valentin@iunona.pmf.ukim.edu.mk.

<sup>†</sup> Université de Bretagne Occidentale.

<sup>‡</sup> Institute of Chemistry, "Sv. Kiril i Metodij" University.

<sup>§</sup> Institute of Biology, "Sv. Kiril i Metodij" University.

<sup>||</sup> University in Greifswald.

**SCHEME 1: Schematic Representation of the Three-Phase Paraffin-Impregnated Graphite Electrode<sup>a</sup>**

<sup>a</sup> The organic solvent that contains a neutral redox probe is attached to the electrode surface as a macroscopic droplet.

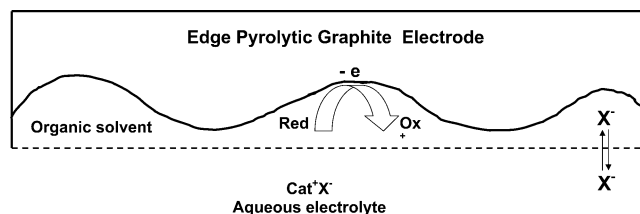
transfer of various anions from water to nitrobenzene can be studied. Besides nitrobenzene, 1,2-dichloroethane,<sup>9</sup> octanol,<sup>10</sup> and menthol<sup>11</sup> can be utilized as organic solvents in combination with PIGE. Note that the latter two organic solvents cannot be used in the conventional experiment based on a four-electrode arrangement<sup>12</sup> because nonsuitable electrolytes can be found to get a polarizable interface. To study the transfer of cations from water to nitrobenzene, reducible redox probes were used such as iodine<sup>13</sup> or iron(III) tetraphenylporphyrin chloride.<sup>14</sup>

A few attempts have been made to assemble the three-phase electrode using electrode materials other than PIGE. Marken et al. used a basal plane pyrolytic graphite electrode modified with spatially distributed microdroplets of 4-(3-phenylpropyl)-pyridine containing cobalt tetraphenylporphyrin as a redox probe.<sup>15</sup> Recently, we developed a new three-phase electrode system consisting of an edge pyrolytic graphite electrode (EPGE) modified with a NB solution of lutetium bis(tetra-*tert*-butylphthalocyaninato) (LBPC).<sup>5</sup> The properties of the latter redox compound appear to be superior to all previously used redox probes in the three-phase electrode system. Its hydrophobicity and chemical stability are significantly higher than other redox probes used so far in the three-phase system. Moreover, LBPC can be both oxidized and reduced in a reversible one-electron step, yielding chemically stable hydrophobic cations and anions, respectively.<sup>16</sup> Hence, this sort of a three-phase electrode was used to interrogate the transfer of anions and cations from water to NB in a single voltammetric experiment.<sup>5</sup> The direct transfer of the hydrophilic alkali metal cations from water to NB was demonstrated for the first time without using facilitating agents in the organic phase.<sup>5</sup>

It is interesting to note that the wetting properties of PIGE and EPGE with organic solvents are considerably different. For instance, nitrobenzene solution, deposited on PIGE, forms a macroscopic semispherical droplet, whereas it spreads spontaneously on the surface of EPGE, forming a thin film.

Having different types of working electrodes and redox probes, it is a challenge to compare their properties in order to provide a deeper insight into the complex coupled electron-ion transfer processes at the three-phase electrode. The first objective of the current study is to compare the behavior of three-phase PIGE and EPGE electrodes using DMFC and LBPC as redox probes, to clarify the role of the redox probes and the type of the electrode material as well as to inspect the mass transfer regime.

Besides the application of the three-phase electrode to measure the thermodynamics of the ion transfer, an attempt is made to develop a methodology for assessing the kinetics of the ion transfer across the L|L interface.<sup>17–22</sup> Recently, we reported on experiments providing kinetic information on the ion transfer using a graphite electrode completely covered with

**SCHEME 2: Schematic Representation of the Three-Phase Pyrolytic Graphite Electrode<sup>a</sup>**

<sup>a</sup> The scheme shows the possible microstructure of a part of the electrode covered with an uneven film of an organic solvent that contains a neutral redox probe.

a thin organic film containing a redox probe and a suitable electrolyte.<sup>23</sup> However, the main constraint of this methodology is the presence of an electrolyte in the organic phase, which limits considerably the number of accessible ions. In the present study, it is demonstrated that the three-phase electrode can also be utilized for kinetic measurements of ion transfer. This is of particular importance inasmuch the three-phase electrode enables a study of a large number of ions that are inaccessible by the conventional four-electrode arrangement.

## 2. Experimental Section

LBPC was synthesized and purified according to the procedure already described.<sup>16,24</sup> DMFC was a product of Fluka. All other chemicals and nitrobenzene were of high purity and used as received. Both LBPC and DMFC were dissolved in water-saturated nitrobenzene (2 mmol/L).

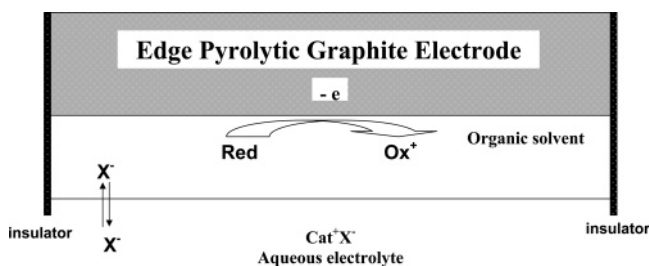
The paraffin-impregnated graphite electrode (PIGE) is a graphite rod with a 0.5 cm diameter and an exposed surface area of 0.2 cm<sup>2</sup>. Before depositing the organic solution, the electrode was abraded with SiC paper (600) and polished on a white paper. A 1  $\mu$ L portion of the nitrobenzene solution containing a redox probe was attached as a single semispherical droplet to the surface of PIGE by the help of a pipet (Scheme 1). If the electrode was not polished on a white paper, its surface could be wetted with a minute amount of nitrobenzene solution ( $\sim 0.2$   $\mu$ L), which forms a thin film or spatially distributed microdroplets.

The other type of working electrode was a disk (0.32 cm<sup>2</sup>) of oriented pyrolytic graphite with the edge planes exposed to the aqueous solution (EPGE). The preparation of the electrode is described elsewhere.<sup>23</sup> Nitrobenzene solution spreads spontaneously over this electrode surface, forming a very thin film. Using a minute amount of nitrobenzene solution (0.2  $\mu$ L), the film does not cover the electrode surface completely; thus, a three-phase boundary is formed (Scheme 2). Due to the roughness of the graphite electrode and the very low thickness of the organic phase, the organic film has an uneven structure. This type of electrode configuration is called three-phase EPGE.

After the deposition of 1  $\mu$ L of nitrobenzene solution, the electrode surface is completely covered, and this sort of electrode configuration will be referred to as thin-film-modified EPGE (Scheme 3).

Square-wave and cyclic voltammograms were recorded using PGSTAT 12 equipment (Eco-Chemie, Utrecht, Netherlands). A saturated calomel electrode or a Ag|AgCl|saturated NaCl electrode was used as the reference and a platinum wire as the auxiliary electrode. Water (Millipore Q) was saturated with nitrobenzene to prevent dissolution of the organic solvent in the aqueous phase. All experiments were performed at room temperature.

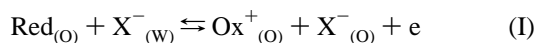
**SCHEME 3: Schematic Representation of the Pyrolytic Graphite Electrode Modified with an Even Thin Film of an Organic Solvent that Covers the Electrode Surface Completely<sup>a</sup>**



<sup>a</sup> The organic solvent contains a neutral redox probe.

### 3. Results and Discussion

**3.1. Comparative Study of the Thermodynamics of the Ion Transfer Using Three-Phase Electrodes.** Using a neutral lipophilic redox probe such as DMFC<sup>2</sup> or LBPC,<sup>5</sup> which both can be oxidized to a stable monovalent cation in the organic phase, the electron transfer process at the three-phase electrode is assumed to be coupled by a charge compensating anion  $X^-$  transfer from the aqueous phase to the organic phase. In the absence of any chemical interaction between the redox probe and the transferring ion, the overall process is described by the following reaction:



with the formal potential defined as<sup>2</sup>

$$E_c^\theta = E_{\text{Ox}_{(\text{O})}^+|\text{Red}_{(\text{O})}}^\theta + \Delta_{\text{w}}^{\text{O}}\varphi_{X^-}^\theta - \frac{RT}{T} \ln(a_{X_{(\text{w})}^-}) + \frac{RT}{F} \ln\left(\frac{a_{\text{Red}_{(\text{O})}}^*}{2}\right) \quad (1)$$

Here,  $E_{\text{Ox}_{(\text{O})}^+|\text{Red}_{(\text{O})}}^\theta$  is the standard potential of the redox couple in the organic phase,  $\Delta_{\text{w}}^{\text{O}}\varphi_{X^-}^\theta$  is the standard potential of the transfer of  $X^-$  from water to the organic phase, and  $a_{\text{Red}_{(\text{O})}}^*$  is the bulk activity of the redox probe in the organic phase. Equation 1 is valid only for the conditions  $a_{\text{Red}_{(\text{O})}}^* \ll a_{X_{(\text{w})}^-}^*$ .<sup>25</sup> The electrochemical transformation of the redox probe at the graphite|organic solution interface serves as the driving force for the ion transfer across the aqueous electrolyte|organic solution interface. It means that the thermodynamic data derived on the basis of eq 1, that is, the standard potential of the ion transfer,  $\Delta_{\text{w}}^{\text{O}}\varphi_{X^-}^\theta$ , should be independent of the redox probe used in the three-phase electrode experiment; that is, there is no ion-pair formation or complex association.

Figure 1A shows the dependence of the net SW peak potential,  $E_p$ , on the standard potential of the anion transfer,  $\Delta_{\text{w}}^{\text{O}}\varphi_{X^-}^\theta$ , measured by the oxidation of DMFC (curve 1) and LBPC (curve 2), at the three-phase PIGE. In both cases, an excellent linear dependence was obtained associated with a regression coefficient of  $R = 0.996$  and  $0.997$  for DMFC and LBPC, respectively. The slopes are  $0.996$  (DMFC) and  $1.01$  (LBPC), being in very good agreement with the theoretical value 1, predicted by eq 1.

The dependence of the peak potential on the aqueous concentration of the transferring ion was inspected using  $\text{NO}_3^-$ . The peak potential depends linearly on  $\log(c_{\text{NO}_3^-})$  ( $R = 0.999$  for both redox probes) with a slope of  $-53$  and  $-50$  mV for DMFC and LBPC, respectively, which is in close agreement

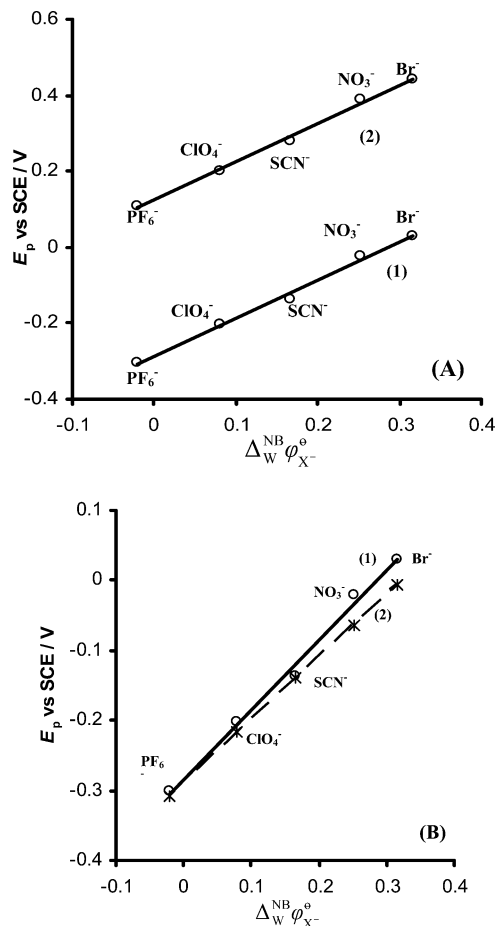


**Figure 1.** (A) Influence of the transferring ion on the net SW peak potential of the three-phase PIGE using DMFC (1) and LBPC (2) as a redox probe. (B) Influence of the transferring ion on the net SW peak potential of the three-phase PIGE (1) and EPGE (2) using DMFC as a redox probe. The concentration of the aqueous electrolytes and the redox probe was  $0.1$  mol/L and  $2$  mmol/L. The parameters of the potential modulation were the following: frequency,  $f = 8$  Hz; amplitude,  $E_{\text{sw}} = 50$  mV; and step of the staircase ramp,  $dE = 0.15$  mV.

with eq 1. These results show that the thermodynamic properties of the anion transfer are independent of the redox probe, at least when DMFC or LBPC is used.

To inspect the influence of the electrode material, a comparative study has been carried out using a three-phase PIGE and a three-phase EPGE and DMFC as a redox probe (Figure 1B). Although the configurations of these two types of electrodes are different (Schemes 1 and 2), the dependence  $E_p$  versus  $\Delta_{\text{w}}^{\text{O}}\varphi_{X^-}^\theta$  is quite similar for both electrodes. There is only a slight difference in the slope of the lines, the values being  $0.997$  and  $0.894$  for PIGE and EPGE, respectively (Figure 1B). This difference could be explained considering the effect of the partition of the aqueous electrolyte. In the case of the three-phase EPGE (Scheme 2), the partition of the aqueous electrolyte may have progressed deeper into the organic film, due to its low thickness. As a consequence, the concentration of the transferring ion provided by partition in the organic phase could slightly affect the overall equilibrium at the formal potential of the system. A considerable free partition of the aqueous salt will lead to a violation of the basis preconditions made in the derivation of eq 1. At the three-phase PIGE, this effect is insignificant, due to the macroscopic dimension of the droplet, implying that this type of three-phase electrode is favorable for assessing the thermodynamics of the ion transfer.



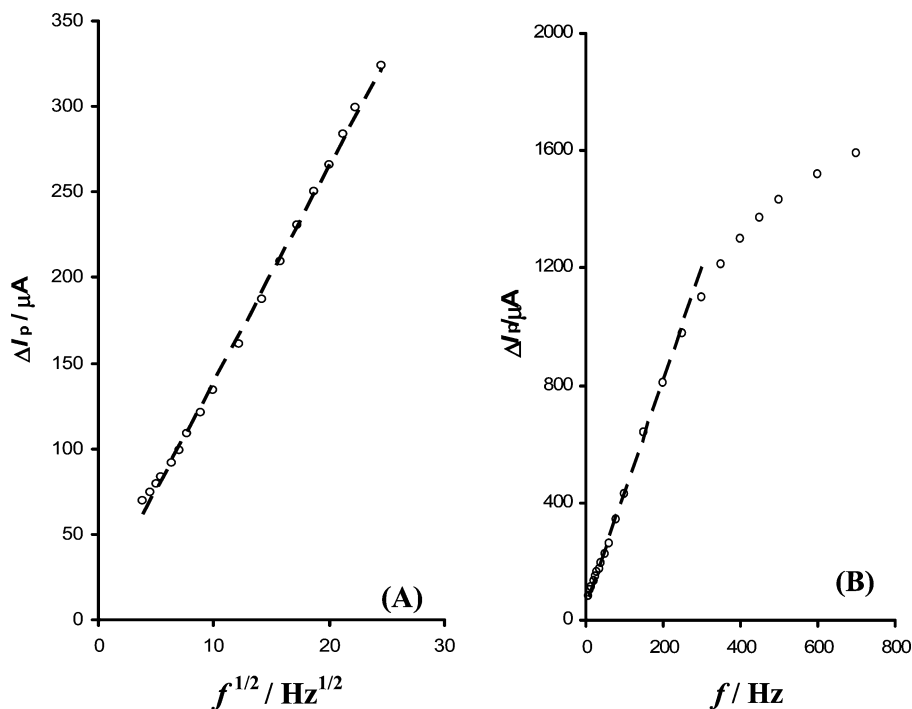


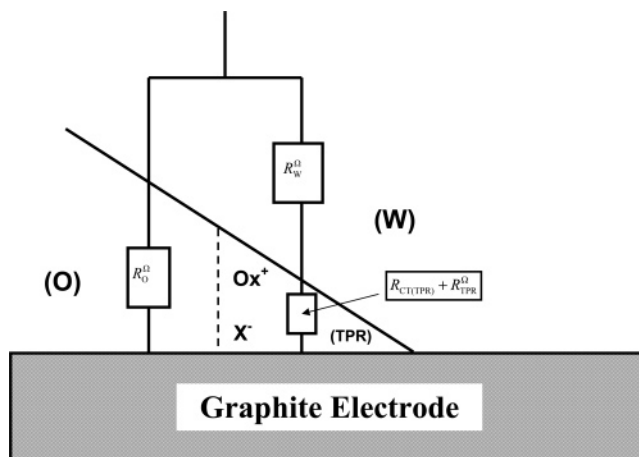
**Figure 2.** Effect of the SW frequency on the net peak current of SW voltammograms for the oxidation of DMFC recorded at the three-phase PIGE (A) and EPGE (B) in contact with a 0.5 mol/L aqueous solution of  $\text{KNO}_3$ . The other conditions are the same as those in Figure 1.

Significant differences in the behavior of the two electrodes were observed by varying the frequency of the potential modulation. Over the frequency interval  $15 \leq f/\text{Hz} \leq 600$ , the net peak current measured at the three-phase PIGE depends linearly on the square root of the frequency, which is typical for electrode reactions where the mass transport occurs as semi-infinite diffusion<sup>26</sup> (Figure 2A). At the same time, the peak potential and the half-peak width of the net SW response are only slightly affected by the frequency. An increase of the frequency from 15 to 600 Hz caused the peak potential to shift in the positive direction for 7 mV and the half-peak width to enhance for 5 mV. These results show clearly that the uncompensated resistance does not influence the SW response<sup>6</sup> and the mass transfer regime occurs by semi-infinite diffusion of the electroactive species.<sup>25</sup> It is interesting to emphasize that the ratio of the net peak current and the square root of the frequency,  $\Delta I_p f^{-1/2}$ , decreases monotonically from 17.94 to  $13.23 \mu A \text{ Hz}^{-1/2}$  by increasing the frequency from 15 to 600 Hz, respectively. This result indicates that the system is under kinetic control of the coupled electron–ion transfer reaction at the three-phase electrode. Note that the ratio  $\Delta I_p f^{-1/2}$  is independent of the frequency for a reversible reaction.<sup>26</sup>

In contrast to the PIGE, the response measured at the three-phase EPGE is characterized by a linear dependence of the net peak current on the frequency, over the interval  $15 \leq f/\text{Hz} \leq 250$  (Figure 2B). This is typical for an electrode reaction in thin-film voltammetry.<sup>25</sup> Above 250 Hz, a strong deviation from linearity occurs, indicating the influence of the charge transfer kinetics (Figure 2B). By increasing the frequency from 15 to 700 Hz, the peak potential shifts in the positive direction for 3 mV and the half-peak width increases for 11 mV. Interestingly, the ratio  $I_p f^{-1/2}$  is a parabolic function. This is an intrinsic property of a kinetically controlled reaction in thin-film voltammetry,<sup>27</sup> which will be elaborated in more detail.

Important conclusions can be derived on the basis of the foregoing results. First, both three-phase electrodes are unaffected by ohmic drop of the organic phase. This is because the ohmic drop within the organic phase droplets or organic phase

**SCHEME 4: Schematic Representation of the Resistance of the Organic Phase (O) and the Resistance of the Three-Phase Region<sup>a</sup>**



<sup>a</sup> In the three-phase region, the organic phase contains  $\text{Ox}^+$  and  $\text{X}^-$  species and the distance between the GE|O and O|W interfaces is very small; hence, the Ohmic resistance of the organic phase,  $R_{TPR}^\Omega$ , is very small. The Ohmic resistance of the organic phase containing not yet  $\text{Ox}^+$  and  $\text{X}^-$ , i.e.,  $R_O^\Omega$ , is very high, but it cannot affect the current response because it is in parallel to  $R_W^\Omega$  and  $R_{CT(TPR)} + R_{TPR}^\Omega$  ( $R_{CT(TPR)}$  is the resistance of the charge transfer in the three-phase region, and  $R_W^\Omega$  is the resistance of the aqueous phase that is negligible due to the aqueous electrolyte).

film that has not been converted into a  $\text{DMFC}^+/\text{X}^-$  containing solution is in parallel (not in a series) to the three-phase electrode region where the electrochemistry proceeds (Scheme 4). Second, under conditions of SWV, at higher frequencies, the coupled electron–ion transfer reaction at the three-phase electrode is a kinetically controlled process. Third, the mass transfer at the three-phase PIGE is governed mainly by semi-infinite diffusion, whereas at the three-phase EPGE it occurs in a restricted space.

The analysis carried out with cyclic voltammetry (CV) supports the foregoing conclusions. Figure 3 shows cyclic

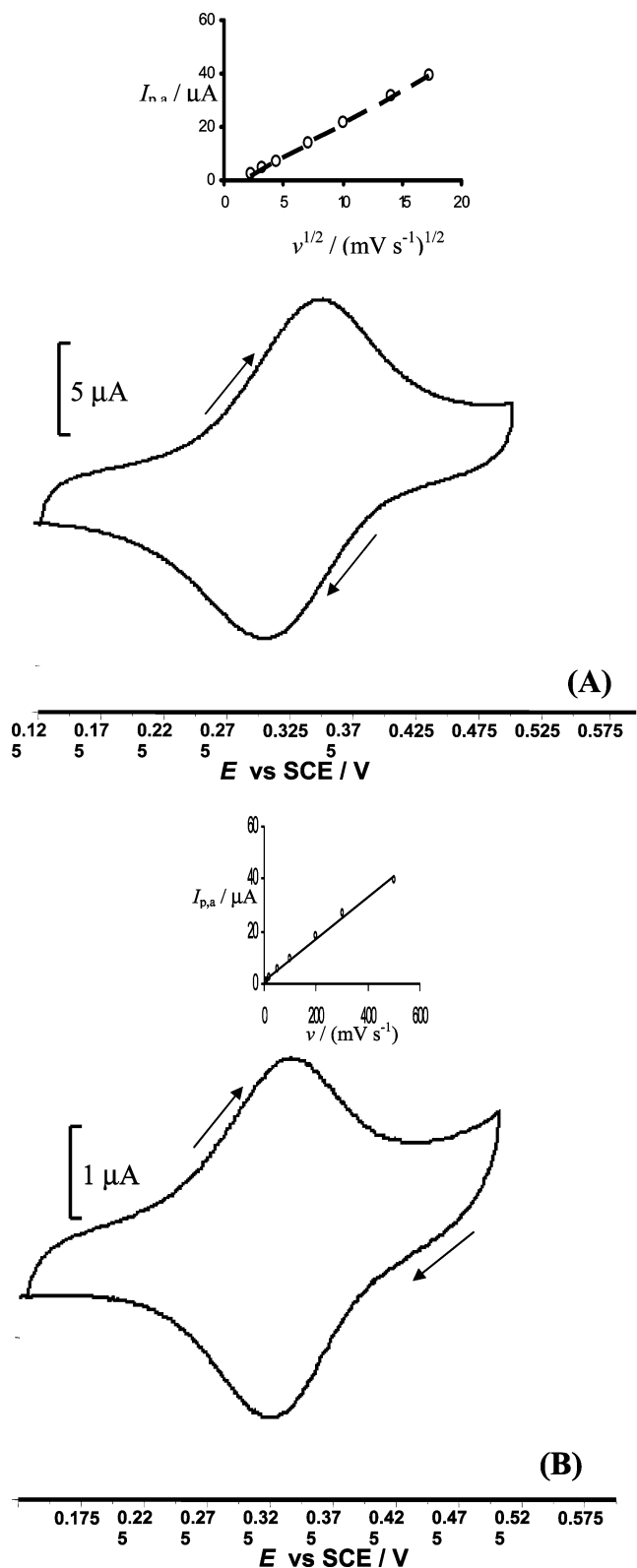


**Figure 3.** Cyclic voltammogram of LBPC recorded at the three-phase PIGE (A) and the three-phase EPGE (B) in contact with a 0.5 mol/L aqueous solution of  $\text{KNO}_3$ . The scan rate was  $10 \text{ mV s}^{-1}$ . The concentration of LBPC in nitrobenzene was 2 mmol/L. The insets show the dependence of the anodic peak current on the square root of the scan rate (A) and the scan rate (B).

voltammograms of LBPC recorded at the three-phase PIGE and EPGE. Both systems are particularly stable under cycling of the potential. The cyclic voltammogram recorded at the three-phase PIGE (Figure 3A) has typical diffusion tails and a peak

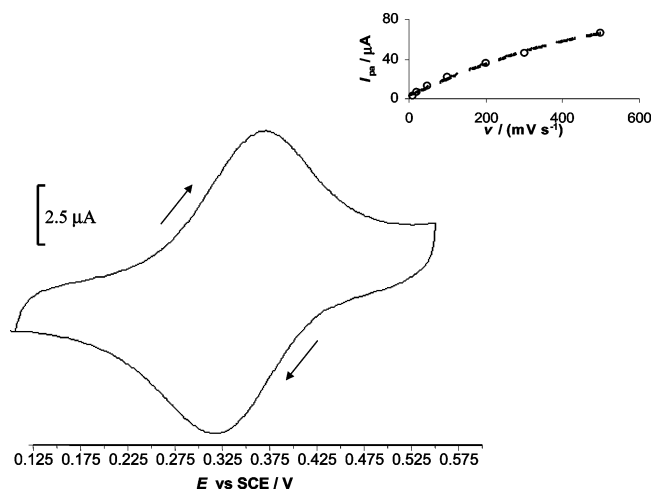


**Figure 4.** Cyclic voltammogram of LBPC recorded at the thin-film-modified EPGE in contact with a 0.5 mol/L aqueous solution of  $\text{KNO}_3$ . The electrode was modified by depositing  $1 \mu\text{L}$  of NB solution containing 2 mmol/L of LBPC. The scan rate was  $10 \text{ mV s}^{-1}$ . The inset shows the dependence of the anodic peak current on the scan rate.

potential separation of  $\Delta E_p = 50 \text{ mV}$ . Moreover, the peak currents depend linearly on the square root of the scan rate (inset of Figure 3A), confirming that the reaction is under semi-infinite diffusion control. The peaks of the cyclic voltammogram recorded at the three-phase EPGE (Figure 3B) are more symmetric compared to the voltammogram recorded at PIGE. Their peak potential separation is only  $\Delta E_p = 11 \text{ mV}$ , whereas the peak currents depend linearly on the scan rate (inset of Figure 3B), which confirms that the process is controlled by the diffusion within the restricted space of the thin film. The shape and properties of the cyclic voltammograms clearly show that the ohmic drop is insignificant in the both three-phase electrode systems. Moreover, the results collected by using the three-phase EPGE imply that this electrode system combines the advantages of the three-phase and thin-film voltammetric experiment.

To reveal the role of the three-phase boundary line, a series of experiments has been carried out using thin-film-modified EPGE<sup>28–30</sup> (Scheme 3), and the results are compared with those of the three-phase EPGE. The thin-film-modified electrode depicted in Scheme 3 differs from the three-phase EPGE (Scheme 2) only in the thickness distribution of the film on the surface. Since no extremely thin regions exist in the case of Scheme 3, the behavior will no longer be describable by the three-phase model.

A cyclic voltammogram of LBPC recorded at the thin-film-modified electrode in contact with a 0.5 mol/L aqueous solution of  $\text{KNO}_3$  is presented in Figure 4. There are significant differences in comparison with the corresponding voltammogram recorded at the three-phase EPGE (compare Figures 4 and 3B), in particular with respect to the peak potential separation. The peak potential separation is 55 and 11 mV for the voltammogram recorded at the thin-film-modified EPGE and the three-phase EPGE, respectively. By increasing the scan rate from 5 to  $1000 \text{ mV s}^{-1}$ , the peak potential separation at the three-phase EPGE enlarges from 7 to 16 mV, whereas in the case of thin-film-modified electrode the separation increases from 24 to 77 mV. Furthermore, the peak current of the cyclic voltammogram recorded at the thin-film-modified EPGE are not a linear function of the scan rate (inset of Figure 4), as expected for the thin-film voltammetric experiment. The latter

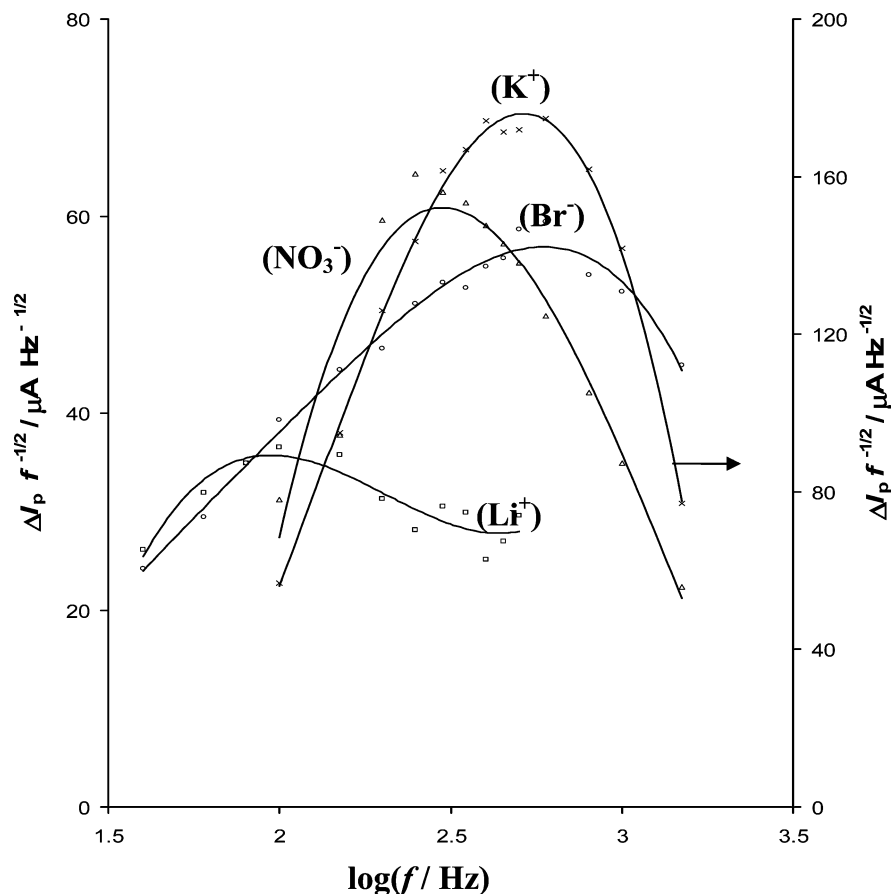


**Figure 5.** Quasireversible maxima recorded by the oxidation and reduction of LBPC at the three-phase EPGE in contact with a 0.5 mol/L aqueous solution of  $\text{KNO}_3$  and  $\text{LiBr}$ . The quasireversible maxima of  $\text{NO}_3^-$  and  $\text{Br}^-$  were recorded by measuring the oxidation of LBPC, whereas the maxima corresponding to the transfer of  $\text{K}^+$  and  $\text{Li}^+$  were measured by the reduction of LBPC.<sup>5</sup> The other conditions are the same as those in Figure 1.

results imply that the ohmic drop is significant at the thin-film-modified EPGE in the absence of an electrolyte in the organic phase.

To check the ability of the thin-film-modified EPGE to measure the standard potential of ion transfer, the net SW peak potential was measured in the presence of different anions in the aqueous phase using DMFC as a redox probe. Under the same experimental conditions as those in Figure 1, the dependence  $E_p$  versus  $\Delta_w \phi_{X^-}^\theta$  is associated with the following regression line:  $E_p/V = 0.996\Delta_w \phi_{X^-}^\theta/V - 0.285$  ( $R = 0.999$ ). In this analysis, the transfer of  $\text{ClO}_4^-$ ,  $\text{SCN}^-$ ,  $\text{NO}_3^-$ , and  $\text{Cl}^-$  was considered. The measurements with the lipophilic  $\text{PF}_6^-$  did not provide reliable results, which was not the case for the three-phase electrode system. Besides, the net SW peak current of the response recorded at the thin-film-modified EPGE exhibited a complex nonlinear dependence on the frequency. The net peak current is not a linear function of either the frequency or the square root of the frequency. All of these results imply that the thin-film-modified EPGE in the absence of an electrolyte in the organic phase suffers from a significant influence of the uncompensated resistance. This effect is almost absent for the three-phase electrode EPGE, which is as a consequence of the very low thickness of the organic film.

**3.2. Application of Three-Phase Electrodes for Assessing the Kinetics of the Ion Transfer Across the L|L Interface.** In a recent theoretical study,<sup>27</sup> it has been predicted that a kinetically controlled electrode reaction in thin-film SW voltammetric experiments exhibits the property known as “quasireversible maximum”. The quasireversible maximum is manifested as a parabolic dependence of the ratio of the net SW

peak current and the square root of the frequency,  $\Delta I_p f^{-1/2}$ , versus the logarithm of the frequency. The maximum of this ratio is reached when the reaction is quasireversible. The quasireversible maximum is an inherent property of a kinetically controlled reaction in thin-film SWV;<sup>27</sup> thus, it can be utilized as a diagnostic criterion for a quasireversible reaction. The position of the maximum depends on the standard rate constant of the charge transfer. The higher the standard rate constant, the higher the critical frequency at which the maximum is positioned. Therefore, the quasireversible maximum can be exploited for assessment of the charge transfer kinetics.

The existence of the quasireversible maximum was experimentally proven in the recent study using EPGE covered completely with the thin film of a nitrobenzene solution containing DMFC or LBPC as redox probes (Scheme 3).<sup>23</sup> The experiments have been performed in the presence of the transferring ion in both liquid phases, the concentration of which was 2 orders of magnitude higher than the redox probe. Provided  $\text{ClO}_4^-$ ,  $\text{NO}_3^-$ , or  $\text{Cl}^-$  was the transferring ion, it has been proven that the coupled electron–ion transfer process is controlled by the kinetics of the ion transfer across the W|NB interface. However, this experimental methodology<sup>23</sup> can be applied to study some ions only, that is, those capable of creating salts that are well soluble in the organic phase. On the other hand, the three-phase electrode provides insight into the transfer of a large series of miscellaneous ions in the absence of an electrolyte in the organic phase. Therefore, it is particularly important to find conditions to measure and to study the quasireversible maximum using the three-phase electrode.

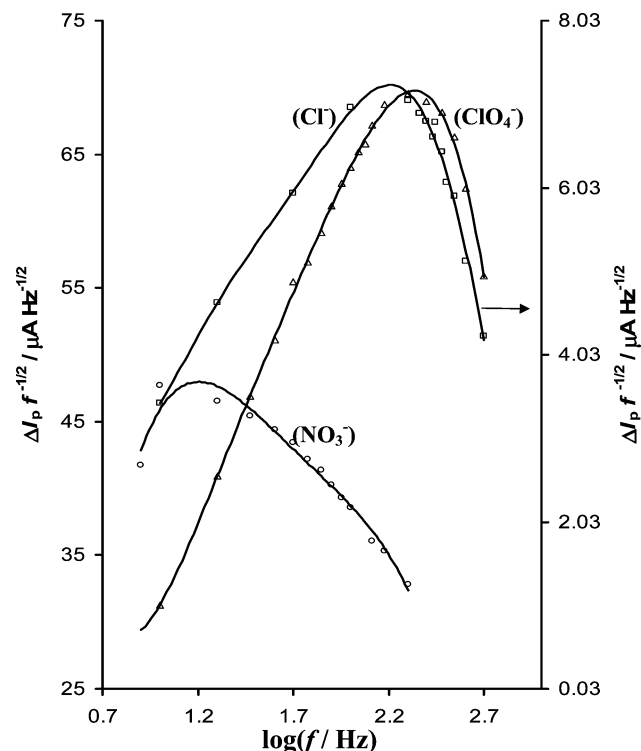


**Figure 6.** Quasireversible maxima recorded at the three-phase PIGE at the surface of which 0.2  $\mu\text{L}$  of nitrobenzene solution containing 1 mmol/L of DMFC was imposed. The quasireversible maxima were recorded in contact with an aqueous solution containing 0.8 mol/L  $\text{KNO}_3$ ,  $\text{NaCl}$ , and  $\text{NaClO}_4$ . The other conditions are the same as those in Figure 1.

Figure 5 shows a series of quasireversible maxima measured at the three-phase EPGE using LBPC as a redox probe. The quasireversible maxima have been measured in 0.5 mol/L aqueous solutions of  $\text{KNO}_3$  and  $\text{LiBr}$  using the oxidation as well as the reduction processes of LBPC. As demonstrated in ref 5, LBPC can be both oxidized and reduced at the three-phase EPGE accompanied by the transfer of an anion and a cation from water to nitrobenzene, respectively. Thus, this redox probe provides insight into the transfer of both anions and cations across the  $\text{W}|\text{NB}$  interface.

The positions of the quasireversible maxima in Figure 5 reveal particularly important information. First, the position of the maximum varies for different transferring ions and the same redox probe, indicating that the process is controlled by the ion transfer kinetics. The critical frequencies for the transfer of  $\text{NO}_3^-$  and  $\text{Br}^-$ , measured by the oxidation of LBPC are  $f_{\text{max}} = 250$  and 500 Hz, respectively. Hence, the transfer of  $\text{Br}^-$  from water to nitrobenzene proceeds at a faster rate than that of  $\text{NO}_3^-$ . The quasireversible maximum corresponding to the transfer of  $\text{K}^+$  and  $\text{Li}^+$ , measured by the reduction of LBPC, is positioned at  $f_{\text{max}} = 450$  and 100 Hz, respectively. The positions of the quasireversible maxima reveal the relative rate of the transfer of studied ions from water to nitrobenzene, which increases in the series  $\text{Li}^+ < \text{NO}_3^- < \text{K}^+ < \text{Br}^-$ .

The quasireversible maxima can also be measured by PIGE, provided the electrode was only abraded on the SiC paper and subsequently wetted with a minute volume of the organic solution (0.2  $\mu\text{L}$ ). Figure 6 shows quasireversible maxima measured for the oxidation of 1 mmol/L DMFC corresponding to the transfer of  $\text{NO}_3^-$ ,  $\text{ClO}_4^-$ , and  $\text{Cl}^-$ . In agreement with the previous data, the type of the transferring ion determines the position of the maximum. The transfer of  $\text{Cl}^-$  proceeds at a faster rate than  $\text{NO}_3^-$ , in accordance with the previous study.<sup>23</sup>

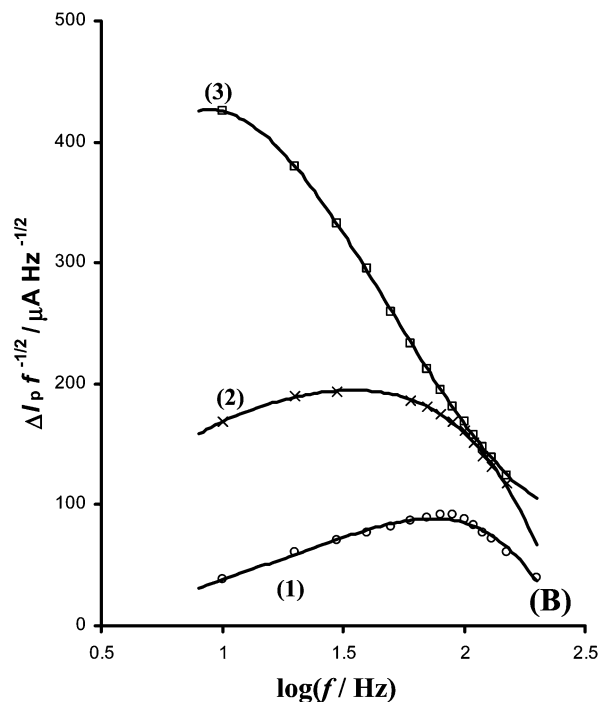
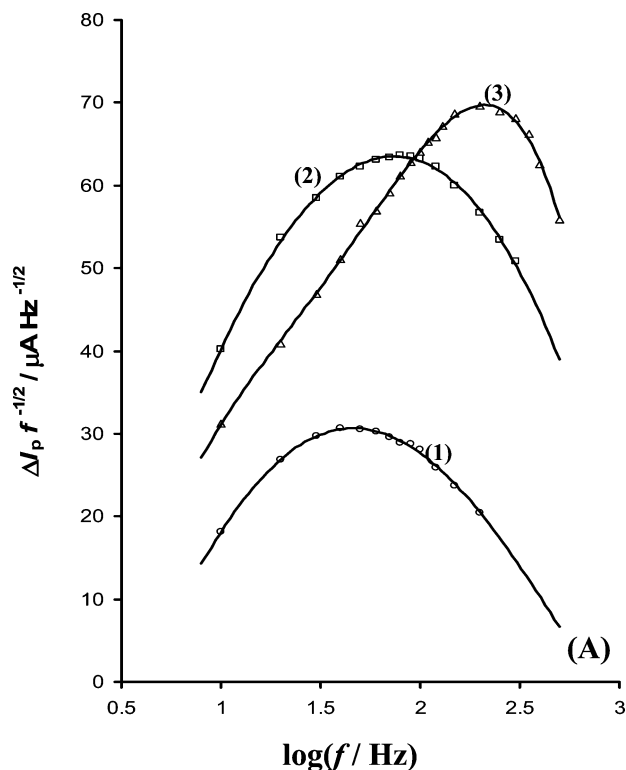


**Figure 7.** Effect of the concentration of the transferring ion (A) and the redox probe (B) on the position of the quasireversible maxima measured by the oxidation of DMFC at the three-phase PIGE in contact with  $\text{NaClO}_4$  aqueous solution. The other conditions for part A were the following: the concentration of  $\text{ClO}_4^-$  in the aqueous solution was 0.1 (1), 0.4 (2), and 0.8 mol/L (3), and the concentration of DMFC in NB was 1 mmol/L. The conditions for part B were the following: the concentration of DMFC in NB was 1 (1), 5 (2), and 10 mmol/L, and the concentration of  $\text{ClO}_4^-$  in the aqueous phase was 0.4 mol/L. The other conditions are the same as those in Figure 1.

It has to be pointed out that, besides the type of the transferring ion, the position of the quasireversible maximum depends on the concentration of both the transferring ion and the redox probe. The evolution of the quasireversible maximum



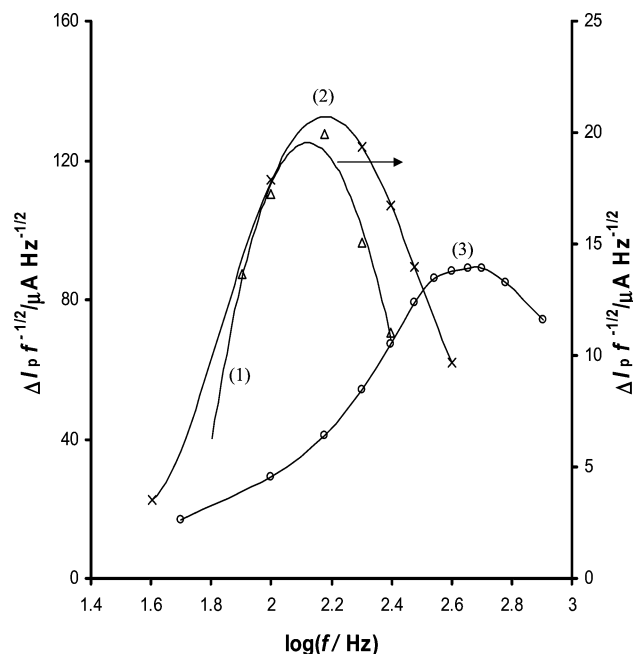


**Figure 8.** Effect of the concentration of the transferring ion on the position of the quasireversible maxima measured by the reduction of LBPC at the three-phase EPGE in contact with  $\text{KNO}_3$  aqueous solution. The concentration of  $\text{K}^+$  ion in the aqueous phase was the following: 0.1 (1), 0.25 (2), and 0.5 mol/L (3). The concentration of LBPC in NB was 2 mmol/L. The other conditions are the same as those in Figure 1.

measured by varying the concentration of the transferring ion in the aqueous phase and the redox probe is presented in Figure 7. Interestingly, an increase of the transferring ion concentration shifts the quasireversible maximum toward higher frequencies (Figure 7A), whereas an increase of the redox probe concentration causes the opposite effect (Figure 7B). The dependence of the quasireversible maximum on both the transferring ion and the redox probe concentration is a consequence of the complex second-order coupled electron–ion transfer reaction occurring at the three-phase electrode (reaction I). In a concurrent publication,<sup>31</sup> it has been shown that the overall properties of reaction I depend on the concentration ratio  $\rho = c_{\text{X(w)}}^*/c_{\text{Red(NB)}}^*$ , where  $c_{\text{X(w)}}^*$  and  $c_{\text{Red(NB)}}^*$  are the bulk concentration of the transferring ion and the redox probe, respectively. The theoretical model revealed that the maximum is shifted toward a higher critical frequency by increasing the concentration ratio, which is in agreement with the present experimental results (Figure 7). Actually, the position of the quasireversible maximum represents the apparent overall rate of the coupled electron–ion transfer process at the three-phase electrode. As the overall rate is controlled by the ion transfer, the increase of the ion concentration results in acceleration of the overall reaction, causing a corresponding shift of the maximum toward a higher frequency.

The same behavior was observed in the evolution of the quasireversible maximum corresponding to the transfer of  $\text{K}^+$  ion measured by the reduction of LBPC (Figure 8). The quasireversible maximum was shifted from 150 to 200 to 500 Hz by increasing the  $\text{K}^+$  concentration from 0.1 to 0.25 to 0.5 mol/L, which confirms that the process is controlled by the transfer rate of  $\text{K}^+$  from water to nitrobenzene.

In this first attempt to apply the three-phase electrode for kinetic measurements, it is demonstrated that the coupled electron–ion transfer reaction is kinetically controlled under conditions of SWV, attributed with the quasireversible maximum. The position of the quasireversible maximum, which represents the kinetics of the overall process, is sensitive to the

type and concentration of the transferring ion, implying that the kinetics is controlled by the ion transfer across the L|L interface. For exact estimation of the ion transfer kinetics, it is necessary to develop an appropriate theoretical model corresponding to the conditions at the three-phase electrode. Considering the ability of the three-phase electrode to study a large number of ions, this simple methodology is rather promising for measuring the ion transfer kinetics.

#### 4. Conclusion

In this study, it is demonstrated that the three-phase electrode could be assembled as either a paraffin-impregnated graphite electrode modified with a macroscopic droplet of an organic solvent or as an edge plane pyrolytic graphite electrode modified with a very thin uneven film of the organic solvent. Although the organic solvent contains only a neutral redox probe, that is, decamethylferrocene or lutetium bis(tetra-*tert*-butylphthalocyaninato), the coupled electron–ion transfer reaction at the two types of three-phase electrodes proceeds without significant influence of the uncompensated resistance. The thermodynamic properties of the ion transfer across the liquid interface are independent of the type of redox probe used in the organic solvent, demonstrating that no chemical interactions between the transferring ion and the redox probe occur. The main differences between the three-phase electrode consisting of a macroscopic droplet and uneven thin film are with respect to the mass transfer regime within the organic phase.

In square-wave voltammetry, under conditions of a higher frequency of the potential modulation, the coupled electron–ion transfer at the three-phase electrode is a kinetically controlled process, exhibiting the property known as a quasireversible maximum. The overall rate of the coupled electron–ion transfer process is dictated by the rate of the ion transfer. It is demonstrated for the first time that the three-phase electrode in combination with the quasireversible maximum is a new tool for assessing the kinetics of ion transfer across the L|L interface.

**Acknowledgment.** The authors thank A. Pondaven for the preparation of the lutetium complex; V.M. acknowledges gratefully the financial support of both Université de Bretagne Occidentale and A. v. Humboldt-Stiftung.

#### References and Notes

- (1) *Liquid Interfaces in Chemical, Biological, and Pharmaceutical Applications*; Volkov, A. G., Ed.; Marcel Dekker: New York, Basel, 2001.
- (2) Scholz, F.; Komorsky-Lovrić, Š.; Lovrić, M. *Electrochem. Commun.* **2000**, *2*, 112–118.
- (3) Komorsky-Lovrić, Š.; Riedl, K.; Gulaboski, R.; Mirčeski, V.; Scholz, F. *Langmuir* **2002**, *18*, 8000–8005.
- (4) Bouchard, G.; Galland, A.; Carrupt, P.-A.; Gulaboski, R.; Mirčeski, V.; Scholz, F.; Girault, H. *Phys. Chem. Chem. Phys.* **2003**, *5*, 3748–3751.
- (5) Quentel, F.; Mirčeski, V.; L'Her, M. *J. Phys. Chem. B* **2005**, *109*, 1262–1267.
- (6) Mirčeski, V.; Gulaboski, R.; Scholz, F. *J. Electroanal. Chem.* **2004**, *566*, 351–360.
- (7) Donten, M.; Stojek, Z.; Scholz, F. *Electrochem. Commun.* **2002**, *4*, 324–329.
- (8) Komorsky-Lovrić, Š.; Mirčeski, V.; Kabbe, Ch.; Scholz, F. *J. Electroanal. Chem.* **2004**, *566*, 371–377.
- (9) Komorsky-Lovrić, Š.; Lovrić, M.; Scholz, F. *J. Electroanal. Chem.* **2001**, *508*, 129–137.
- (10) Gulaboski, R.; Mirčeski, V.; Scholz, F. *Electrochem. Commun.* **2002**, *4*, 277–283.
- (11) Scholz, F.; Gulaboski, R.; Mirčeski, V.; Langer, P. *Electrochem. Commun.* **2002**, *4*, 659–662.
- (12) Girault, H. H.; Schiffrin, D. J. In *Electroanalytical Chemistry*; Bard, A. J., Ed.; Marcel Dekker: New York, 1989; Vol. 15, pp 1–141.
- (13) Mirčeski, V.; Gulaboski, R.; Scholz, F. *Electrochem. Commun.* **2002**, *4*, 814–819.

- (14) Scholz, F.; Gulaboski, R.; Caban, K. *Electrochem. Commun.* **2003**, *5*, 929–934.
- (15) Marken, F.; McKenzie, K. J.; Shul, G.; Opallo, M. *Faraday Discuss.* **2005**, *129*, 1–11.
- (16) L'Her, M.; Pondaven, A. Electrochemistry of phthalocyanines. In *The Porphyrin Handbook. Phthalocyanines: Spectroscopic and Electrochemical Characterization*; Kadish, K., Guillard, R., Smith, K., Eds.; Academic Press: 2003; Vol. 16, pp 117–170.
- (17) Samec, Z. In *Liquid–Liquid Interfaces. Theory and Methods*; Volkov, A. G., Deamer, D. W., Eds.; CRC Press: 1996; pp 155–178.
- (18) Manzanares, J. A.; Allen, R. M.; Kontturi, K. *J. Electroanal. Chem.* **2000**, *483*, 188–196.
- (19) Murtomaki, L.; Kontturi, K.; Schiffrin, D. J. *J. Electroanal. Chem.* **1999**, *474*, 89–93.
- (20) Samec, Z.; Langmaier, J.; Trojanek, A. *J. Electroanal. Chem.* **1999**, *463*, 232–241.
- (21) Manzanares, J. A.; Lahtinen, R.; Quinn, B.; Kontturi, K.; Schiffrin, D. J. *Electrochim. Acta* **1998**, *44*, 59–71.
- (22) Buck, R. P.; Bronner, W. E. *J. Electroanal. Chem.* **1986**, *197*, 179–181.
- (23) Quentel, F.; Mirčeski, V.; L'Her, M. *Anal. Chem.* **2005**, *77*, 1940–1949.
- (24) Pondaven, A.; Cozien, Y.; L'Her, M. *New J. Chem.* **1992**, *16*, 711–718.
- (25) Komorsky-Lovrić, Š.; Lovrić, M.; Scholz, F. *Collect. Czech. Chem. Commun.* **2001**, *66*, 434–444.
- (26) Lovrić, M. In *Electroanalytical methods, Guide to experiments and applications*; Scholz, F., Ed.; Springer-Verlag: Berlin, Heidelberg, 2002; pp 111–133.
- (27) Mirčeski, V. *J. Phys. Chem. B* **2004**, *108*, 13719–13725.
- (28) Shi, C.; Anson, C. F. *Anal. Chem.* **1998**, *70*, 3114–3118.
- (29) Shi, C.; Anson, C. F. *J. Phys. Chem. B* **1998**, *102*, 9850–9854.
- (30) Shi, C.; Anson, C. F. *J. Phys. Chem. B* **1999**, *103*, 6283–6289.
- (31) Quentel, F.; Mirčeski, V.; L'Her, M.; Scholz, F., submitted.